Journal of Immunotoxicology

ISSN: 1547-691X (Print) 1547-6901 (Online) Journal homepage: informahealthcare.com/journals/iimt20

A comparison of neurodegeneration linked with neuroinflammation in different brain areas of rats after intracerebroventricular colchicine injection

Susmita Sil, Rupsa Ghosh, Moumita Sanyal, Debjani Guha & Tusharkanti Ghosh

To cite this article: Susmita Sil, Rupsa Ghosh, Moumita Sanyal, Debjani Guha & Tusharkanti Ghosh (2016) A comparison of neurodegeneration linked with neuroinflammation in different brain areas of rats after intracerebroventricular colchicine injection, Journal of Immunotoxicology, 13:2, 181-190, DOI: 10.3109/1547691X.2015.1030804

To link to this article: https://doi.org/10.3109/1547691X.2015.1030804

Published online: 27 Mar 2015.

Journal of Immunotoxicology

http://www.tandfonline.com/iimt
ISSN: 1547-691X (print), 1547-6901 (electronic)
J Immunotoxicol, 2016; 13(2): 181–190

DOI: 10.3109/1547691X.2015.1030804

Taylor & Francis
Taylor & Francis Group

RESEARCH ARTICLE

A comparison of neurodegeneration linked with neuroinflammation in different brain areas of rats after intracerebroventricular colchicine injection

Susmita Sil[1], Rupsa Ghosh[1], Moumita Sanyal[1], Debjani Guha[2], and Tusharkanti Ghosh[1]

[1]*Department of Physiology, University College of Science and Technology and* [2]*S. N. Pradhan Centre for Neurosciences, University of Calcutta, West Bengal, India*

Abstract

Colchicine induces neurodegeneration, but the extent of neurodegeneration in different areas of the brain in relation to neuroinflammation remains unclear. Such information may be useful to allow for the development of a model to compare colchicine-induced neurodegeneration with other neurodegenerative diseases such as Alzheimer's Disease (AD). The present study was designed to investigate the extent of neurodegeneration along with neuroinflammation in different areas of the brain, e.g. frontal cortex, parietal cortex, occipital cortex, corpus striatum, amygdala and hippocampus, in rats along with memory impairment 21 days after a single intracerebroventricular (icv) injection of colchicine. Memory parameters were measured before and after icv colchicine injection in all test groups of rats (control, sham-operated, colchicine-injected [ICIR] rats). On Day 21 post-injection, rats from all groups were anesthesized and tissues from the various brain areas were collected for assessment of biomarkers of neuroinflammation (i.e. levels of ROS, nitrite and proinflammatory cytokines TNFα and IL-1β) and neurodegeneration (assessed histologically). The single injection of colchicine resulted in impaired memory and neurodegeneration (significant presence of plaques, Nissl granule chromatolysis) in various brain areas (frontal cortex, amygdala, parietal cortex, corpus striatum), with maximum severity in the hippocampus. While IL-1β, TNFα, ROS and nitrite levels were altered in different brain areas in the ICIR rats, these parameters had their greatest change in the hippocampus. This study showed that icv injection of colchicine caused strong neurodegeneration and neuroinflammation in the hippocampus of rats and the increases in neurodegeneration were corroborated with those of neuroinflammation at the site. The present study also showed that the extent of neurodegeneration and neuroinflammation in different brain areas of the colchicine-injected rats were AD-like and supported the fact that such rats might have the ability to serve as a sporadic model of AD.

Keywords

Colchicine, hippocampus, neurodegeneration, neuroinflammation

History

Received 30 December 2014
Revised 25 February 2015
Accepted 15 March 2015
Published online 1 April 2015

Introduction

Colchicine is an alkaloid (Alali et al., 2004), derived from the seeds of *Colchicum autumnale* plants (Shibli et al., 2010), which have been known for more than 2000 years for their marked beneficial and poisonous effects (Brickell, 1984). Besides its medicinal use in gout (Terkeltaub, 2003) and Mediterranean fever (Drenth & van der Meer, 2001), colchicine is also used in biological studies and breeding (Trease & Evans, 1989). It is also known as a ''mitotic poison'', since it inhibits microtubule polymerization, resulting in inhibition of spindle formation during mitosis (Shibli et al., 2010).

Colchicine is also reported to be neurotoxic as it binds with tau proteins, resulting in disruption of microtubules (Emerich & Walsh, 1990; Wilson, 1986). As a result, axoplasmic flow is affected and normal activity of the neuron gets seriously jeopardized in a manner that may result in neuronal death (Emerich & Walsh, 1990; Wilson, 1986). It was reported that, within 3 h after colchicine administration, amyloid precursor protein (APP) was found to accumulate in proximal axons that eventually come out from the cell (Koo et al., 1990). In the axon, APP has been shown to move by fast anterograde axonal transport. Aberrant accumulation of APP in neurons of the CNS, particularly in proximal axons, may be caused by disturbances of fast axonal flow. This APP may accumulate outside the cell after the neuronal death and may give rise to plaques.

Degenerating neurons and plaques generate inflammatory mediators that may activate microglia and astrocytes which generate several neurotoxic cytokines (interleukin [IL]-1β, IL-6 and tumor necrosis factor [TNF]-α), Reactive oxygen species (ROS) and reactive nitrogen species (RNS) and these cytokines, in turn, further cause increased microglial activation present in the surroundings leading to further neurodegeneration (Aloisi, 2001; Gehrmann et al., 1995; Nyoman & Darmadipura, 2007). In addition, activated microglia attracts neutrophils and monocytes to the CNS (Mallat & Chamak, 1994; Minton, 2001; Streit, 1993)

Address for correspondence: Dr. Tusharkanti Ghosh, Neurophysiology Laboratory, Department of Physiology, University College of Science and Technology, University of Calcutta, 92, Acharya Prafulla Chandra Road, Kolkata 700-009, West Bengal, India. Tel: 919433251974. Fax: 9103323519755. E-mail: tusharkantighosh53@yahoo.in

that adds onto the neurodegeneration by causing increased release of neurotoxic cytokines, as well as of more ROS and RNS (Aloisi, 2001; Gehrmann et al., 1995; Nyoman & Darmadipura, 2007). Thus, ROS, nitrite, TNFα and IL 1β are important biomarkers of neuroinflammation that may be induced by colchicine at the site of neurodegeneration.

Although colchicine-induced neurodegeneration is well known, the extent of neurodegeneration in different areas of the brain after its intracerebroventricular (icv) administration remains to be investigated. The type of information gleaned from those types of studies may be useful to compare colchicine-induced neurodegeneration with that associated with other neurodegenerative diseases, such as Alzheimer's Disease (AD). A colchicine (icv)-induced neurodegeneration model has been considered by many as a sporadic model of AD on the basis of impairment of cognitive functions and loss of cholinergic neurons (Ganguly & Guha, 2008; Kumar et al., 2007a; Pitchaimani et al., 2012; Shigematsu & McGeer, 1992).

However, the histopathological characteristics of changes induced by icv colchicine injection remain ill-defined. One immunohistochemistry study reported that amyloid precursor protein (APP) immunoreactivity in different areas of the brain, e.g. hippocampus, lateral septal nucleus, amygdala, entorhinal, parietal and temporal cortices, was increased after icv colchicine injection (Shigematsu & McGeer, 1992). However, that study did not report the extent of the effect of the colchicine in these different brain areas. Therefore, the present study was designed to investigate the extent of neurodegeneration in different areas of the brain (frontal cortex, parietal cortex, occipital cortex, corpus striatum, amygdala and hippocampus) in icv colchicine-injected rats along with memory impairment in these animals. Biomarkers of neuroinflammation related to neurodegeneration, such as levels of ROS, nitrite and proinflammatory cytokines (like TNFα and IL-1β) were assessed in the different brain areas as well in order to potentially corroborate the neurodegeneration results with those for neuroinflammation.

Materials and methods

Animals

Charles-Foster rats (male, 200–250 g, 6–8-weeks-of-age) were obtained from a local animal supplier (M/s Chakraborty Enterprise, Kolkata, India) for this study. Rats were housed individually in polypropylene cages in a facility maintained at $25 \pm 1\,^{\circ}C$ with a 12-h light–dark cycle. All rats had *ad libitum* access to standard rodent chow food pellets and filtered water. All rats were acclimated for 1 week prior to use in any study. The institutional Animal Ethics Committee approved all protocols used herein.

Experimental design

Rats were randomly divided into three groups ($n = 6$/group): control (C), sham-operated (receiving only vehicle; S) or intracerebroventricular (icv) colchicine-injected rats (ICIR).

For assessment of memory (see details below), after the initial 1 week acclimation period, all rats were habituated in a radial arm maze (RAM) for 5 days, trained for a further 15 days and then had their memory parameters (number of re-entries in baited arms and number of entries in unbaited arms) measured over 5 days to establish baseline values prior to any treatment with test material. These memory parameters were again tested on Days 9, 12, 15, 18 and 21 after the host treatment. Apart from being of use in assessing trends of effects of treatment on overall memory patterns, the Day 21 data was also used for corroboration with results of the analyses of neurodegeneration and neuroinflammation in biosamples that were to also be collected on Day 21.

To obtain the biosamples on Day 21, all rats were anesthesized with ether (Nandkrishna Chemicals Pvt. Ltd, Mumbai, India). This specific timepoint was selected based on results from a previous study wherein icv colchicine-injected rats were compared for extent on neurodegeneration and neuroinflammation in the brain at Days 15 and 21 post-icv injection (note: effects were seen to be maximum at Day 21 (Sil et al., 2014)). At necropsy, samples from the frontal cortex, parietal cortex, occipital cortex, corpus striatum, amygdala and hippocampus were collected. These were then either processed for histologic analyses of plaques and Nissl granules (i.e. fixation, dehydration, paraffin block preparation, section cutting and staining) or for assessment of ROS, nitrite, TNFα and IL-1β levels.

Intracerebroventricular (icv) injection

Colchicine (7.5 µg in 2.5 µl of artificial CSF) was injected into the lateral ventricle of each side of the rat brain using stereotaxic coordinates: AP at -0.6 mm from bregma; L at ± 1.5 mm from midline; and V at 2.8 mm from the skull surface (Paxinos & Watson, 1986). The rat was anesthetized with Na-thiopentone (50 mg/kg BW, i.p.) and its head fixed on the stereotaxic apparatus (ST141, INCO Ambala, India) with the help of ear bars, an incisor bar and a noseclip. The skull was then opened by midline incision and the periostium (over skull surface) retracted. Burr holes were then made using a dental drill on two points over the skull surface (right and left side) – according to the AP and L coordinates. A steel micro-cannula (0.45-mm diameter) connected to a 10 µl syringe (Hamilton, Reno, NV) with polyethylene tubing, was then inserted into the lateral ventricle using the V coordinate. The cannula was left in place 2–3 min after the injection and then the burr hole was then covered with sterile bone wax. The muscles and skin were then sutured separately and Neosporin powder was sprayed over the cut area as an antiseptic measure. Rats in the sham group received 2.5 µl of artificial CSF (Kumar et al., 2007a) on each side of the brain in the same manner.

Memory testing via radial arm maze (RAM) task

Habituation session

A rat was placed in the central octagonal platform of the RAM kept on a wooden platform in a brightly lit room and allowed to move freely in the connected arms (Wooden, $18.5 \times 3.5 \times 10.5$ in) in which chocolate chips were spread about. The rats were removed from the maze after visiting *all* eight arms (one trial). After each trial the RAM was cleaned with alcohol to remove trace odors of the rewards. Habituation was carried out in a schedule of three trials/day for 5 days, with each trial separated by 2 h. During habituation, the rats were food-deprived to $\approx$ 30% of their normal daily dietary intake.

Training session

After habituation, the rats were trained in a schedule of three trials/day for 15 days. In these sessions, only four selected arms were baited with chocolate and the task was to make the correct arm choice to get the food reinforcement (reward). The rat was made to learn and memorize the particular arms in order to obtain the reward. In the first few trials, the food was kept just at the proximal part of each selected arm. Then the food was moved to the middle of the arm for the next few trials. At the later trials (after 7 days of training), the food was placed at the distal end of the arm so the rat memorized the arm well.

Test trials

Following training, the rats were tested in each of the next 5 days (three trials/day, with 2 h between trials). This established baseline values of memory for each rat prior to any treatment. Each trial consisted of maximum 5 min duration or ended earlier if/when a rat had visited (and consumed reward in) all four baited arms. The same four arms were baited for each trial. All the trials were videotaped and coded. Two observers then independently evaluated the following parameters:

- *Number of re-entries in baited arms*: if a rat re-entered a baited arm, it was considered as an error. The total number of re-entries in the baited arms (considered an indicator of working memory error (Mizuno et al., 2000)) for a rat in a trial (5 min duration or earlier as mentioned above) was recorded; and
- *Number of entries in non-baited arms*: if a rat entered a non-baited arm, it was considered an error (i.e. indicator of reference memory error). The total number of entries in all non-baited arms for one rat in a trial (5 min duration or earlier as mentioned above) was recorded. These memory parameters were again tested on all rats at post-treatment days 9, 12, 15, 18 and 21.

Cytokine assessments in tissues

TNFα

TNFα levels in different areas of the brain were assayed using a Rat TNF-Flex Set and a BD Cytometric Bead Array (CBA) Rat Soluble Protein Master Buffer kit (BD Biosciences, San Jose, CA) in a BD Verse FACS instrument. In all cases, FCAP Array software was used for data analysis. Sample preparation was done according to the method of Csolle & Sperlagh (2010, 2011). In brief, isolated brain areas were homogenized separately in 500 µl of 10 mM Tris-HCl buffer containing 1 mM EGTA, 1 mM EDTA, 0.2 mM PMSF and 4 M urea per 0.1 g tissue. The samples were then centrifuged (15 000 x g, 4 °C, 20 min) and the resultant supernatant collected. A sample (25 µl) of this material was then assessed for protein content using the method of Lowry et al. (1951), with bovine serum albumin (BSA) as the standard. An additional sample (400 µl) was then mixed with 500 µl of a solution containing 10 mM Tris-HCl buffer, 1% BSA and 0.2% Tween-20. An aliquot (50 µl) of this solution was then used to assay TNFα levels, according to manufacturer protocols. Cytokine levels were expressed as pg TNFα/100 mg protein in the sample.

IL-1β

IL-1β levels in different areas of the brain were assayed using a commercial rat IL-1β ELISA Kit (Ray Bio, Norcross, GA). For these analyses, 100 µl of the solutions prepared above were used to assay IL-1β levels, according to manufacturer protocols. In this case, the sample content was based on measures of absorbance at 450 nm/well in a 96 well plate reader (Ray Bio). Cytokine levels were expressed as pg IL-1β/mg protein in the sample. The sensitivity of the kit was 80 pg IL-1β/ml.

ROS estimation

Reactive oxygen species (ROS) in isolated brain areas were estimated using the method of Socci et al. (1999). In brief, a sample of the brain areas were homogenized in 500 µl of ice-cold 40 mM Tris–HCl buffer (pH 7.4) and centrifuged. An aliquot of the resultant supernatant (10 µl) was then combined with 50 µl of a 5 µM DCF-DA solution (Loba Cheme, Mumbai) and incubated for 30 min at 37 °C. Formation of fluorescent DCF was then measured in an FP6200 spectroflurometer (Jasco Inc., Easton, MD) at an excitation wavelength of 495 nm and emission wavelength of 529 nm. ROS present in the sample was expressed as a percentage of control (i.e. mean levels found in control rat tissue samples).

Nitrite estimation

Nitrite levels in the tissue samples were estimated by the method of Green et al. (1982). In brief, 10 µl sample supernatant (from same material generated for ROS assay) was mixed with an equal volume of Griess reagent [0.1% *N*-(1-naphthyl)-ethylenediamine dihydrochloride, 1% sulfanilamide, 2.5% phosphoric acid] and incubated at 37 °C for 10 min. Sample absorbance at 550 nm was then measured in a spectrophotometer (BioRad, Hercules, CA). Nitrite values were expressed as a percentage of control (i.e. mean levels found in control rat tissue samples).

Histological study

Cresyl violet staining for Nissl granules

Nissl granules in the neurons of paraffin brain sections were stained with cresyl violet acetate (Sigma, St. Louis, MO) (Cox, 1977). In brief, the sections were de-paraffinized, dehydrated and then treated with water. The slides were then incubated in cresyl violet (1%) for 20–30 min. After rinsing with distilled water, the slide was treated with 96% alcohol and then absolute alcohol. The dehydrated section was then mounted with DPX and the intensity of Nissl granules was measured using Image J Launcher software (v1.4.3.67; NIH, Bethesda, MD). A total of six microscopic fields/brain area was examined per rat. The mean value of intensity of Nissl granules present/field of the brain area/animal was calculated from the six rats/regimen.

Congo red staining

Plaques in the neurons of paraffin brain sections were stained with Congo red (Central Drug House, India) (Stevens & Bancroft, 1977). In brief, the sections were de-paraffinized, dehydrated and then treated with water. The sections were then stained with Gill's hematoxylin and rinsed in tap water for 2 min before being immersed in alkaline sodium chloride solution for 20 min. The slides were then incubated in Congo red working solution (1% Congo red stock solution) for 20 min. After rinsing the section with distilled water, the material was differentiated with alkaline alcohol and again rinsed in distilled water. The sections were then dehydrated, mounted with DPX and examined under a light microscope. The number of plaques in each brain area of an animal was counted, with 10 microscopic fields/brain area examined. Mean value of plaques/per animal was calculated from the six rats/group and presented graphically.

The intensity of Nissl granules and number of plaques of an animal were measured at the level of AP 3.2 mm for the frontal cortex, AP = 3.3 mm for the parietal cortex, AP = 7.3 mm for the occipital cortex, AP = 1.2 mm for the corpus striatum, AP = 4.8 mm for the hippocampus, and AP = 3.3 mm for the amygdala. The squared dimensions of the sampled fields were 5 mm^2 for each brain area.

Statistics

All data were expressed as mean ± SEM. Memory parameters of rats in each group were analyzed using a one-way analysis of variance (ANOVA) followed by a *post-hoc* Tukey's Multiple Comparison test. For other data, a two-way ANOVA was employed to compare among the different groups (control, sham-operated, ICIR) and across different brain regions. This was followed by a one-way ANOVA and a Tukey's Multiple Comparison test to compare the data of the control,

sham-operated and ICIR of each brain region with another. All analyses were performed using SPSS software (v.20, Cary, NC).

Results

Memory parameters

Memory impairment in the ICIR rats was indicated by changes in the number of re-entries in baited arms and in the number of entries in unbaited arms of the RAM system. The mean number of re-entries in baited arms and number of entries in unbaited arms by the ICIR rats were significantly increased ($p<0.001$) from Day 9 to Day 21 compared to that of time-matched control (C) and sham-operated (S) rats. Overall, in the ICIR hosts, there was a gradual increase of both of these parameters in a time-related manner after the single icv colchicine injection. Among the C and S rats, the number of re-entries in baited arms and entries in unbaited arms was not significantly changed at any point up to Day 21 or on Day 21 (Table 1).

Intensity of Nissl granules

The intensity of Nissl granules in all of the observed brain areas (hippocampus, frontal cortex, amygdala, parietal cortex and corpus striatum) was significantly lower ($p<0.001$) in ICIR except occipital cortex than that of the respective areas in the control (C) and sham-operated (S) rats. When different brain regions of the ICIR rats were analyzed, it was found that the Nissl granule intensity in the hippocampus and frontal cortex was significantly lower ($p<0.001$) than that seen in the amygdala, corpus striatum, occipital cortex; further, the granule intensity in the parietal cortex was significantly lower ($p<0.001$) in comparison to that in the corpus striatum. On the other hand, in C and S rats, granule intensity in the hippocampus was significantly higher ($p<0.01$) than that in the frontal, parietal and occipital cortex. However, in these rats, Nissl granule intensity did not significantly differ among the hippocampus, frontal cortex and corpus striatum regions. The intensity of Nissl granules in any one of the observed brain areas of C rats did not significantly differ from that of the respective brain areas in the S rats (Figures 1–3).

Numbers of plaques

The number of plaques in the hippocampus was significantly increased ($p<0.001$) in ICIR compared to that of the amygdala, frontal cortex, parietal cortex and corpus striatum. The number of plaques in the amygdala was also significantly increased in ICIR compared to levels seen in the parietal cortex ($p<0.01$) or corpus striatum ($p<0.001$). No plaques were observed in the different brain areas of the C or S rats (Figures 4–6).

TNFα levels

TNFα levels in the hippocampus ($p<0.001$), amygdala ($p<0.001$) and frontal cortex ($p<0.05$) of ICIR rats was significantly higher than of the respective area in C and S rats. TNFα levels in the parietal cortex, occipital cortex and corpus striatum in ICIR rats was not significantly changed from that of the respective area in C and S counterparts. When different brain regions within the ICIR rats were compared, it was found that the TNFα levels in the hippocampus and amygdala were significantly higher ($p<0.001$) than in the frontal, parietal and occipital cortex and in the corpus striatum. In C and S rats, TNFα levels did not significantly differ among any of the brain areas. The TNFα level in any one of the studied brain areas of the C rats did not significantly differ from that of the respective brain area in the S rats (Figure 7).

IL-1β levels

IL-1β levels in the hippocampus of ICIR rats were significantly higher ($p<0.001$) than of the C and S rats. IL-1β levels in the frontal, parietal and occipital cortex, as well as the amygdala and corpus striatum in the ICIR rats did not significantly differ from values in those areas in C and S rats. It was found that, in the different brain regions of the ICIR rats, the IL 1β levels in the hippocampus were significantly higher ($p<0.001$) than that in the amygdala, corpus striatum, frontal, parietal or occipital cortex and that IL 1β levels in the parietal cortex were significantly higher ($p<0.05$) in comparison to in the corpus striatum and occipital cortex. In the C and S rats, the IL 1β level in the hippocampus was significantly lower than that of frontal ($p<0.05$) and parietal cortex ($p<0.01$). However, in C and S rats, the IL 1β levels did not significantly differ among the hippocampus, amygdala, corpus striatum and occipital cortex. IL-1β levels in any one of the studied brain areas of C rats did not significantly differ from that of the respective brain area in S rats (Figure 8).

ROS levels

ROS levels in the hippocampus of ICIR rats were significantly higher ($p<0.001$) than in the C and S rats. ROS levels in the frontal cortex, parietal cortex, occipital cortex, amygdala and corpus striatum in ICIR rats did not significantly differ from that in the respective areas in the C and S counterparts. In the ICIR rats, ROS levels in the hippocampus were significantly higher ($p<0.001$) than in the amygdala, corpus striatum, frontal, parietal and occipital cortex. The ROS levels in any one of the observed brain areas of C rats did not significantly differ from that of the respective brain area in the S rats (Figure 9).

Nitrite levels

The nitrite levels in the hippocampus of ICIR rats were significantly higher ($p<0.001$) than in the C and S rats. The nitrite levels in the amygdala, frontal, parietal and occipital cortex, as well as the corpus striatum in ICIR rats, was not significantly changed compared to values in the same areas in the

Table 1. Memory parameter measures for the ICIR rats.

	ICIR rats					
		Post-injection				
Memory parameters	Pre-injection Days 1–5	Day 9	Day 12	Day 15	Day 18	Day 21
Re-Entries: bited arms (Errors)	0	8.00 ± 0.01^{a}	8.58 ± 0.01^{a}	$9.72\pm0.02^{a,c}$	$11.76\pm0.09^{a,b}$	$15.36\pm0.53^{a,b}$
Entries: unbited arms (Errors)	0	4.80 ± 0.20^{d}	$10.23\pm0.21^{d,c}$	$17.00\pm0.37^{d,c}$	$19.70\pm0.43^{d,c}$	$25.24\pm1.53^{d,c}$

Values at all timepoints for S and C rats were 0. Values shown are mean ± SEM ($n=6$/group).

Number of re-entries in baited arms: [a]Significant difference ($p<0.001$) from pre-injection values for ICIR or for time-matched C or S rats; [b,c]significant difference ([b]$p<0.001$, [c]$p<0.05$) from previous timepoint value.

Number of entries in unbaited arms: [d]Significant difference ($p<0.001$) from pre-injection values for ICIR or for time-matched C or S rats; [e]significant difference ($p<0.001$) from previous timepoint value.

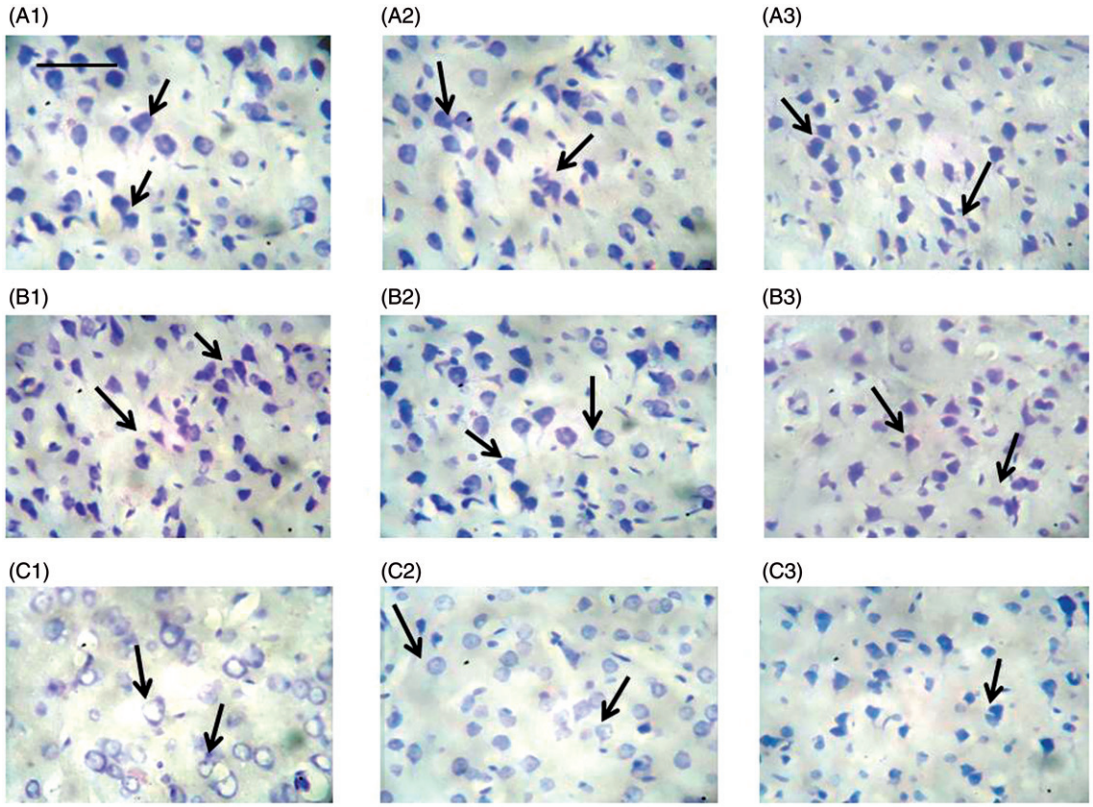

Figure 1. Nissl (cresyl violet) staining of neurons in different brain areas in rats. Representative micrographs are shown. Control rats: (A) (top row); sham-operated rats: (B) (middle row); ICIR [icv colchicine injected]: (C) (last row). Frontal cortex: 1 (left column), parietal cortex: 2 (middle column), occipital cortex: 3 (right column). Letter and number indicate group and specific brain region (e.g. A1: Frontal cortex, control rat). Magnification: 400 ×, length of bar = 16.18 μm. Arrows indicate Nissl granules.

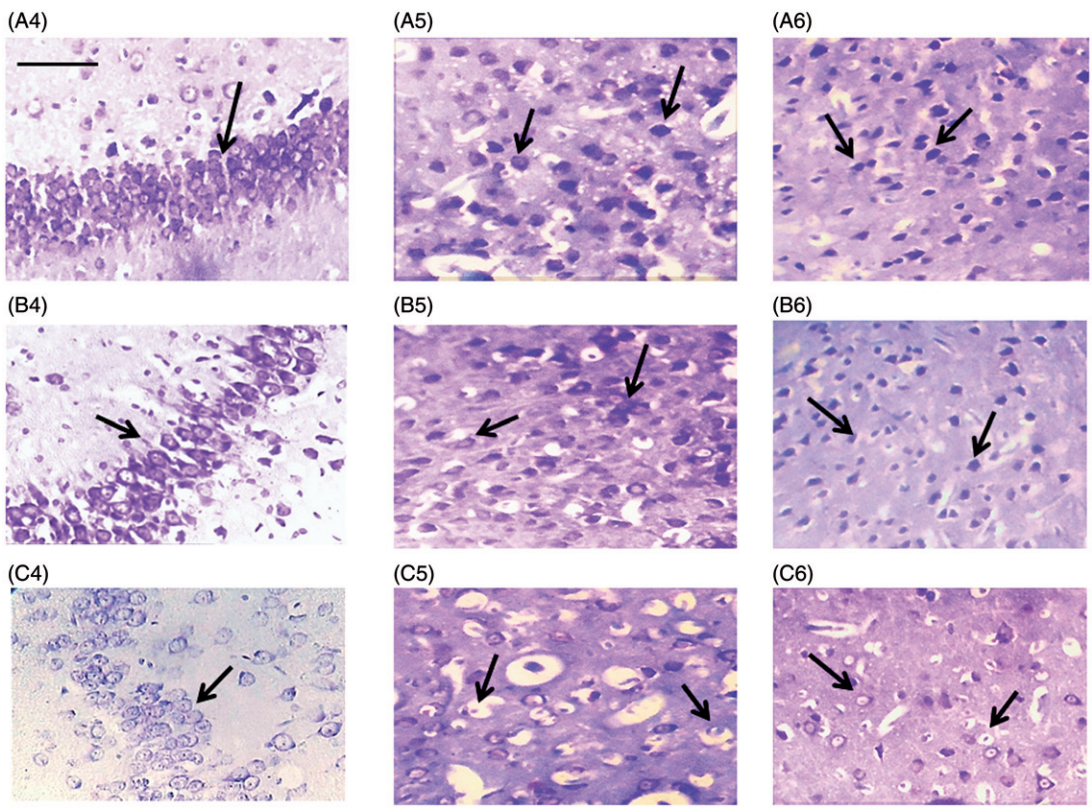

Figure 2. Nissl (cresyl violet) staining of neurons in different brain areas in rats. Representative micrographs are shown. Control rats: (A) (top row); sham-operated rats: (B) (middle row); ICIR [icv colchicine injected] rats: (C) (last row). Hippocampus: 4 (left column), corpus striatum: 5 (middle column), amygdala: 6 (right column). Letter and number indicate group and specific brain region (e.g. A4: Hippocampus, control rat). Magnification: 400 ×, length of bar = 16.18 μm. Arrows indicate Nissl granules.

C and S rats. The results indicated that, in the ICIR rats, nitrite levels in the hippocampus were significantly higher ($p < 0.001$) than those in the amygdala, corpus striatum, frontal, parietal and occipital cortex. The nitrite level in any one of the studies brain areas of the C rats did not significantly differ from that of the respective area in the S rats (Figure 10).

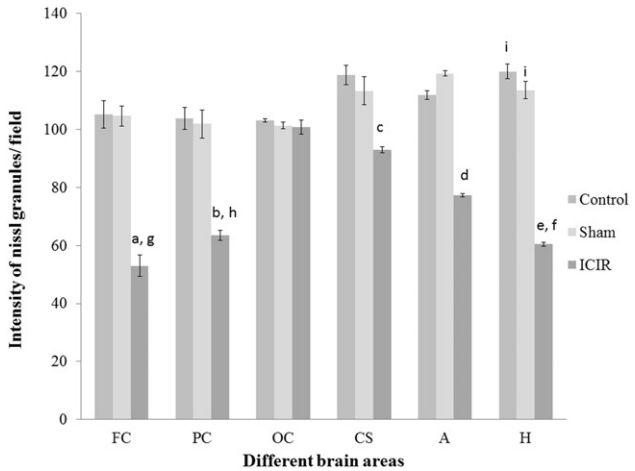

Figure 3. Intensity of Nissl granules in different brain areas of rats. Significant difference ($p < 0.001$) between control (C)/sham-operated (S) rats vs ICIR hosts in (a) frontal cortex, (b) parietal cortex, (c) corpus striatum, (d) amygdala and (e) hippocampus. In ICIR hosts, significant difference ($p < 0.001$) between (f) hippocampus/(g) frontal cortex vs amygdala, corpus stratum, occipital cortex. In ICIR hosts, significant difference ($p < 0.01$) between (h) parietal cortex vs corpus striatum. In control/sham operated hosts, significant difference ($p < 0.01$) between (i) hippocampus vs frontal, parietal and occipital cortex. A,Amygdala; CS, Corpus striatum; FC, Frontal cortex; H, Hippocampus; OC, Occipital cortex; PC, Parietal cortex. Values shown are means ± SEM ($n = 6$/group).

Discussion

In the present study, histopathological changes were analyzed in different brain areas of rats 21 days after a single intracerebroventricular (icv) injection with colchicine. The intensity of Nissl staining in these treated (i.e. ICIR) rats was decreased significantly in the fontal cortex, parietal cortex, amygdala, corpus striatum and hippocampus, from that in the same areas in control and or sham-operated (rats that received icv injection of artificial CSF) rats, indicating chromatolysis in these areas. Within the brains of the ICIR rats, chromatolysis was not similar in all the brain areas, but greater in the hippocampus and frontal cortex compared to in other brain areas. It is probable that chromatolysis was followed by neural death and plaque formation. The presence of increased number of plaques in the hippocampus and frontal cortex can be corroborated with greater chromatolysis in those areas.

Plaques were also observed in other brain regions of ICIR rats: corpus striatum, parietal cortex, frontal cortex and amygdala; however, the number of plaques in the hippocampus was significantly higher (along with maximum chromatolysis) in comparison to in any of the other areas. Neurodegeneration in the hippocampus of ICIR rats has also been observed previously (Roy, 2014; Sil et al., 2014). It should be noted that an increased presence of plaques in the hippocampus and prefrontal cortex (Brun & Englund, 1981; Mouton et al., 1998; Sabuncu et al., 2011) are histological features of mild Alzheimer's disease (AD) and that neurodegeneration spreads out to other areas of the brain with increasing AD severity. In those cases, the greatest neurodegeneration occurs in the hippocampal region and

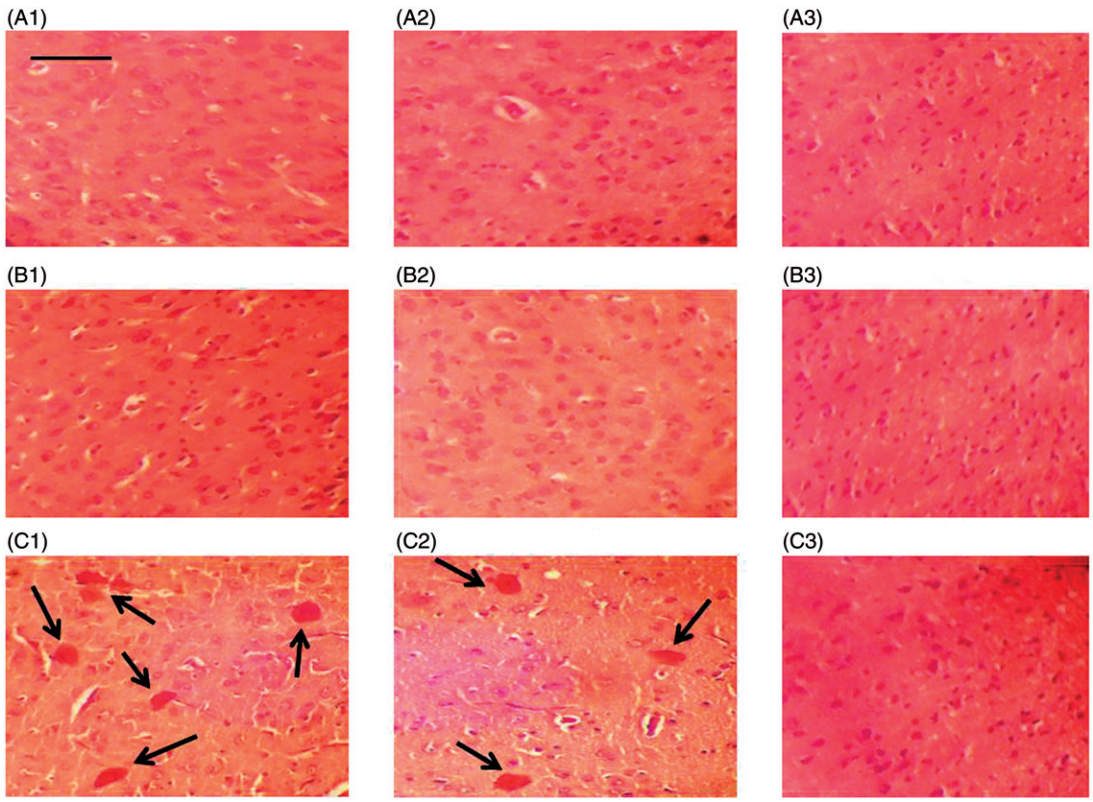

Figure 4. Staining (Congo red) of plaques in different brain areas in rats. Representative micrographs are shown. Control rats: (A) (top row); sham-operated rats: (B) (middle row); icv colchicine injected rats: (C) (last row). Frontal cortex: 1 (left column), parietal cortex: 2 (middle column), occipital cortex: 3 (right column). Letter and number indicate group and specific brain region (e.g, A1: Frontal cortex, control rat). Magnification: 400×, length of bar = 16.18 µm. Arrows indicate plaques.

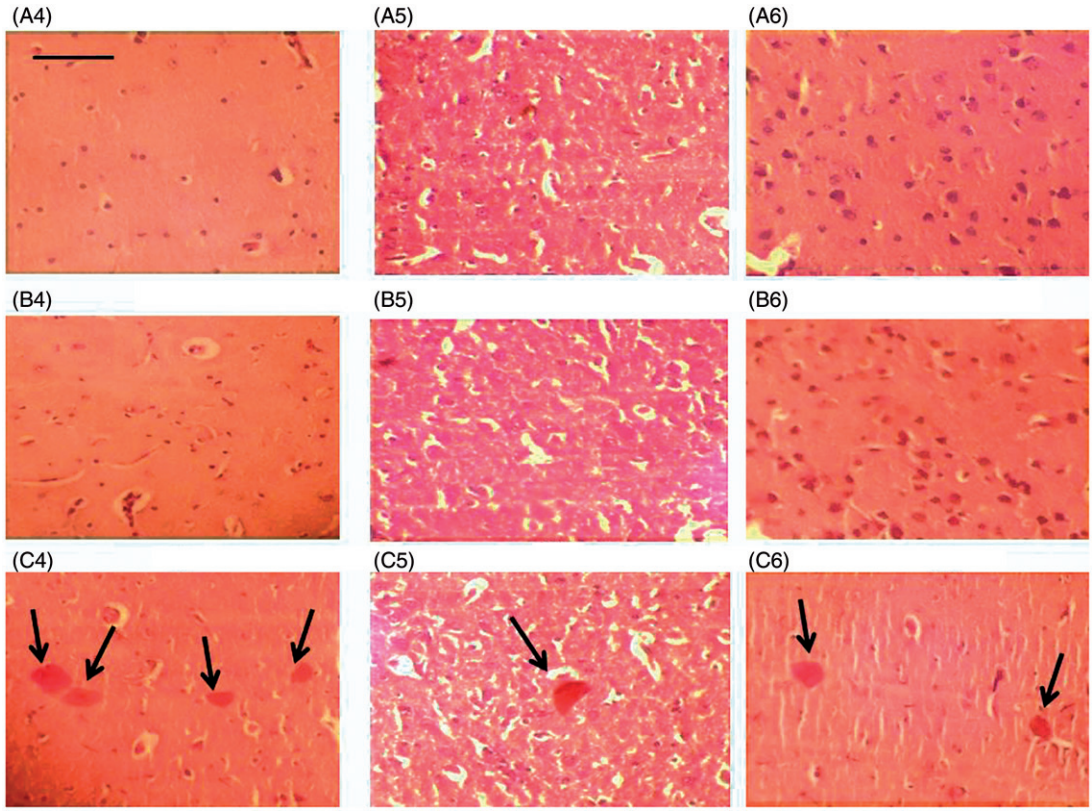

Figure 5. Staining (Congo red) of plaques in different brain areas in rats. Representative micrographs are shown. Control rats: (A) (top row); sham-operated rats: (B) (middle row); icv colchicine injected rats: (C) (last row). Hippocampus: 4 (left column), corpus striatum: 5 (middle column), amygdala: 6 (right column). Letter and number indicate group and specific brain region (e.g. A4: Hippocampus, control rat). Magnification: 400×, length of bar = 16.18 μm. Arrows indicate plaques.

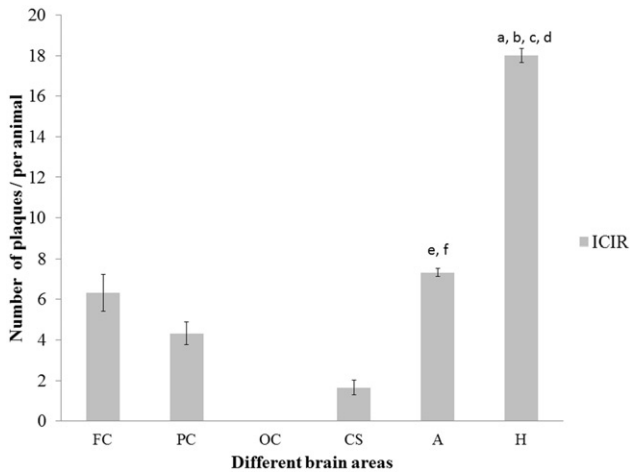

Figure 6. Number of plaques in different brain areas of intracerebroventricular colchicine injected rats (ICIR). Significant difference ($p < 0.001$) between hippocampus vs (a) frontal cortex; (b) parietal cortex; (c) corpus striatum; and (d) amygdala. Significant at $p < 0.001$ between amygdala vs (e) parietal cortex or (f) corpus striatum in ICIR hosts. Values shown are means ± SEM ($n = 6$/group). Abbreviations are as outlined in legend to Figure 3.

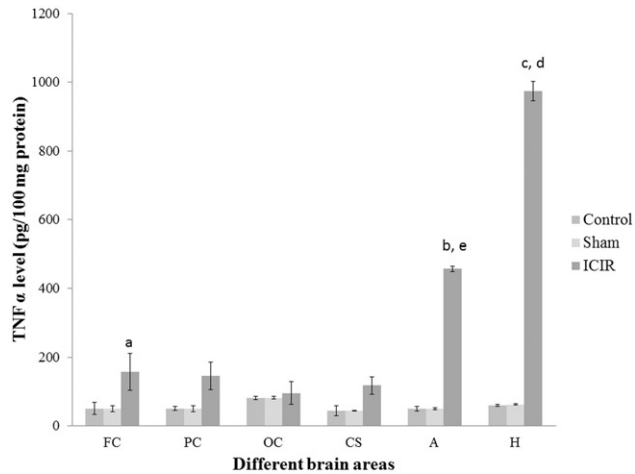

Figure 7. TNFα levels in different brain areas of rats. Significant difference between control (C)/sham-operated (S) rats vs ICIR hosts in (a) frontal cortex ($p < 0.05$), (b) amygdala ($p < 0.001$) and (c) hippocampus ($p < 0.001$). Significant difference ($p < 0.001$) between (d) hippo-campus/(e) amygdala vs frontal cortex, parietal cortex, occipital cortex and corpus striatum in ICIR hosts. Values shown are means ± SEM ($n = 6$/group). Abbreviations are as outlined in legend to Figure 3.

prefrontal cortex. The present study also showed there was a similar trend of neurodegeneration in the ICIR rats, with maximal damage in the hippocampus among the observed brain areas. In AD patients, neurodegeneration was also observed in other areas of the brain, i.e. amyloid plaques were observed in the corpus striatum (Brilliant et al., 2003), parietal cortex (Jacobs et al., 2012) and atrophy of the amygdala was noted in MRI studies (Cuenod et al., 1993).

One reason for the apparent greater effect in the hippocampus of the ICIR rats could be due to the fact that an icv injection of colchicine may easily have affected adjoining areas of lateral ventricles, such as in the hippocampus. The outcomes seen could also be due to a generalized greater sensitivity of hippocampal neurons to colchicine. In fact, the initial exposure of the hippocampus to the higher concentration of colchicine during

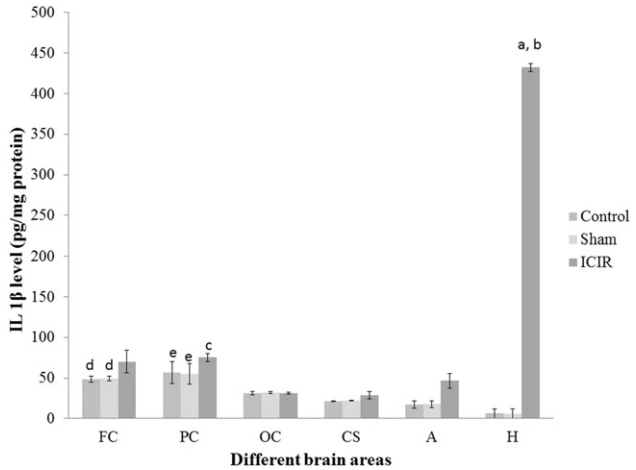

Figure 8. IL 1β levels in different brain areas of rats. (a) Significant difference ($p<0.001$) between hippocampus levels in C and S rats vs in ICIR hosts. (b) Significant difference ($p<0.001$) between hippocampus vs amygdala, frontal cortex, parietal cortex, occipital cortex and corpus striatum in ICIR hosts. (c) Significant difference ($p<0.05$) between parietal cortex vs corpus striatum and occipital cortex in ICIR hosts. (d) Significant difference ($p<0.05$) between hippocampus vs frontal cortex in control/sham operated rats. (e) Significant difference ($p<0.01$) between hippocampus vs parietal cortex in C and S rats. Values shown are means ± SEM ($n=6$/group). Abbreviations are as outlined in legend to Figure 3.

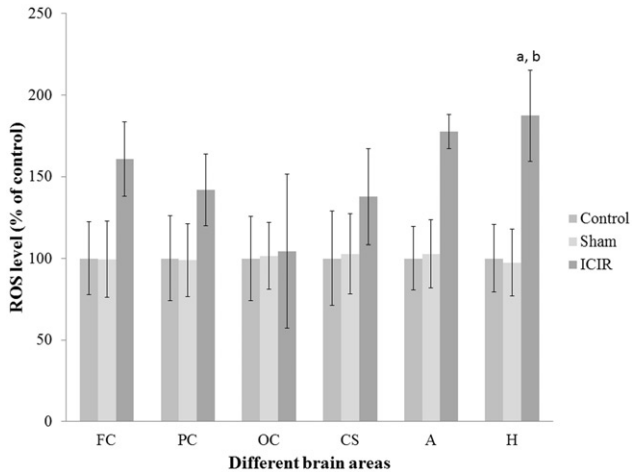

Figure 9. ROS levels in different brain areas of rats. (a) Significant difference ($p<0.001$) between hippocampus levels in C and S rats vs in ICIR hosts. (b) Significant difference ($p<0.001$) between hippocampus vs amygdala, frontal cortex, parietal cortex, occipital cortex and corpus striatum in ICIR hosts. Values shown are means ± SEM ($n=6$/group). Abbreviations are as outlined in legend to Figure 3.

the icv injection may be one reason for higher hippocampal neurodegeneration. Other studies have noted amyloid precursor protein immunoreactivity (indicator of plaques) in the hippocampus, parietal cortex and amygdala in ICIR hosts (Shigematsu & McGeer, 1992), indicating neuronal death in those areas. Thus, the ICIR rats here present with characteristics of neurodegeneration comparable to those noted in AD patients.

The present study also showed that IL-1β and TNFα levels were increased in the hippocampus of the ICIR rats; in the frontal cortex and amygdala, only the level of TNFα was increased in these rats in comparison to the respective brain areas of control and sham-operated counterparts. These outcomes were suggestive of severe inflammation in the hippocampus. It is important to note

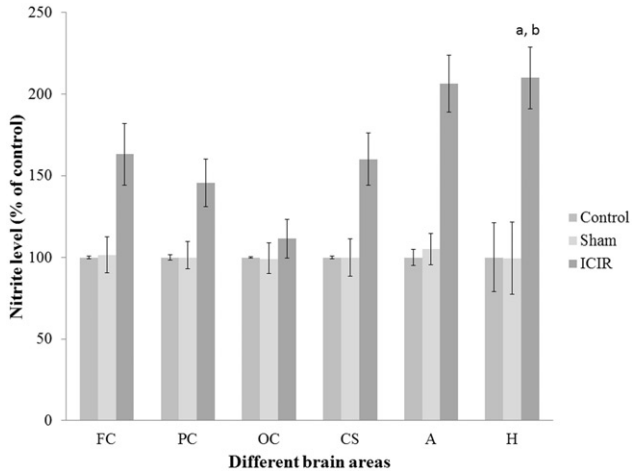

Figure 10. Nitrite levels in different brain areas of rats. (a) Significant difference ($p<0.001$) between hippocampus levels in C and S rats vs in ICIR hosts. (b) Significant difference ($p<0.001$) between hippocampus vs amygdala, frontal cortex, parietal cortex, occipital cortex and corpus striatum in ICIR hosts. Values shown are means ± SEM ($n=6$/group). Abbreviations are as outlined in legend to Figure 3.

that, while TNFα and IL-1β levels in other brain areas of the ICIR rats were not significantly increased, all were still higher compared to the same respective brain areas of the control/sham-operated rats. Further analysis of the data showed that the number of plaques and the percentage decrease in intensity of Nissl granules (taking control/sham as 100%) in the amygdala, frontal cortex, parietal cortex and corpus striatum of ICIR hosts (in addition to in the hippocampus) could be corroborated with the percentage increase (taking value of control/sham as 100%) in inflammatory biomarker (TNFα, IL 1β, ROS, nitrite) levels in these respective brain regions. It is possible that the magnitude of neurodegeneration in different brain areas of these rats were, in fact, dependent on the inflammatory responses induced by colchicine.

Substantial clinical evidence suggests that excess TNFα and IL-1β is somehow involved in the pathogenesis of AD (Bell & Claudio Cuello, 2006). With respect to ROS and nitrite (NO), although levels of these in all the studied brain areas were higher in ICIR rats than in comparable sites in brains of control and sham-operated rats, the only significant increases were again observed only in the hippocampus. In AD patients and in transgenic animal models, it has been reported that oxidative and nitrosative stress is greatest in the hippocampus (Barone et al., 2011; Fanelli et al., 2013; Giuliani et al., 2014). Such findings would be in keeping with the observation of Nolan et al. (2003) who reported that hippocampal cells are more susceptible than cells in other brain regions to degeneration in response to oxidative stress (Nolan et al., 2003). Thus, it is clear that the ICIR rats present characteristics of some of the pathological features associated with AD. Taken together with the histologic findings, this provides further support for our conclusion that the ICIR rat is a good model for studies of AD.

Neurodegeneration in the brains of AD patients are associated with cognitive impairments (Angelucci et al., 2010). Memory parameters in ICIR rats in the present study were evaluated to assess cognitive impairment; using a RAM, the number of re-entries in baited arms by rats was used to assess working memory errors (WME) while reference memory errors (RME) were assessed from the number of entries in unbaited arms (Mizuno et al., 2000). Both of these parameters were impaired in the ICIR hosts here at each post-icv colchicine injection point assessed (i.e. Days 9–21), indicating both WM and RM were affected.

Moreover, the gradual increase in impairment of the two parameters suggested a progressive nature for this impairment, a characteristic feature in AD. The findings here were in line with those of other investigators who showed that icv colchine injection of rats led to impaired memory in a Morris water maze (Kumar & Gupta, 2002; Kumar et al., 2007a, b, 2008, 2010), a step-through passive avoidance apparatus (Pitchaimani et al., 2012) and a radial arm maze (Ganguly & Guha, 2008).

Based on the findings here, we can now postulate a mechanism by which the colchicine acts to bring about the AD-like characteristics in ICIR rats. It was reported earlier that colchicine blocks the axoplasmic flow, resulting in the death of the neurons and plaque formation (Emerich & Walsh, 1990; Sil et al., 2014; Wilson, 1986). In turn, the degenerating neurons release neurotoxic cytokines that activate microglia (Austin & Combs, 2008) and astrocytes that then generate more neurotoxic cytokines (including IL-1β and TNFα), as well as ROS and RNS. These events cause further microglial activation; it is this sustained activation of microglia that results in progressive neurodegeneration (Aloisi, 2001; Gehrmann et al., 1995; Nyoman & Darmadipura, 2007; Rai et al., 2013). The IL-1β, TNFα and ROS/RNS also promote neurodegeneration by up-regulating proinflammatory transcription factor (NF-κB), COX-2 and activating apoptotic pathways (Albrecht et al., 2007; Fan et al., 2008; Figarella et al., 2005; Ke et al., 2007; Parikh et al., 2000).

Conclusion

The present study showed that a single intracerebroventricular injection of colchicine caused maximum neurodegeneration in the hippocampus of rats after 21 days. The same pattern was also observed with respect to the increased presence of proinflammatory cytokines, ROS and nitrite. As such, an increase in neurodegeneration in these ICIR rats can be corroborated with an increase in neuroinflammation in the hippocampus. In the context of disease modeling, the present study showed that the extent of neurodegeneration and neuroinflammation in different brain areas of ICIR rats were AD-like and supports the notion that icv injections of colchicine can yield a suitable rat model of AD.

Acknowledgments

This research work was funded by the University Grant Commission, New Delhi Major Research Project [F. No. 42-532/2013 (SR) dt. 22nd March, 2013]. Dr Sanjay Mallick [Nanoscience and Nanocentre, University of Calcutta] is acknowledged for assistance in some parts of the work.

Declaration of interest

The authors report no conflicts of interest. The authors alone are responsible for the content and writing of the paper.

References

Alali, F., Tawaha, K., and Qasaymeh, R. M. 2004. Determination of colchicine in *Colchicum steveni* and *C. hierosolymitanum* (*Colchicaceae*): Comparison between two analytical methods. *Phytochem. Anal.* 15:27–29.

Albrecht, U., Yang, X., Asselta, R., et al. 2007. Activation of NF-κB by IL-1β blocks IL-6-induced sustained STAT3 activation and STAT3-dependent gene expression of the human gamma-fibrinogen gene. *Cell Signal* 19:1866–1878.

Aloisi, F. 2001. Immune function of microglia. *Glia* 36:165–179.

Angelucci, F., Spalletta, G., di Iulio, F., et al. 2010. Alzheimer's disease (AD) and mild cognitive impairment (MCI) patients are characterized by increased BDNF serum levels. *Curr. Alzheimer Res.* 7:15–20.

Austin, S. A., and Combs, C. K. 2008. Mechanisms of microglial activation by amyloid pre-cursor protein and its proteolytic fragments. In: *Central Nervous System Diseases and Inflammation* (Lane, T.E., Carson, M., Bergmann, C., and Wyss-Coray, T., Eds.). London: Springer, pp. 13–32.

Barone, E., Di Domenico, F., Cenini, G., et al. 2011. Oxidative and nitrosative modifications of biliverdin reductase-A in the brain of subjects with Alzheimer's disease and amnestic mild cognitive impairment. *J. Alzheimers. Dis.* 25:623–633.

Bell, K. F., and Claudio Cuello, A. 2006. Altered synaptic function in Alzheimer's disease. *Eur. J. Pharmacol.* 545:11–21.

Brickell, C. D. 1984. Colchicum L. In: *Flora of Turkey and the East Aegean Islands* (Davis, P.H., ed.). Edinburgh, UK: Edinburgh University Press, pp. 329–351.

Brilliant, M. J., Elble, R. J., Ghobrial, M., and Struble, R. G. 2003. The distribution of amyloid β protein deposition in corpus striatum of patients with Alzheimer's disease. *Neuropathol. Appl. Neurobiol.* 23: 322–325.

Brun, A., and Englund, E. 1981. Regional pattern of degeneration in Alzheimer's disease: Neuronal loss and histopathological grading. *Histopathology* 5:549–564.

Cox, G. 1977. Neuropathological techniques. In: *Theory & Practice of Histological Techniques* (Bancroft, J. D., and Stevens, A., Eds.), London: Elsevier, pp. 258–259.

Csolle, C., and Sperlagh, B. 2010. Peripheral origin of IL-1β production in rodent hippocampus under *in vivo* systemic bacterial lipoplysaccharide (LPS) challenge and regulation by P2X7 receptors. *J. Neuroimmunol.* 219:38–46.

Csölle, C., and Sperlagh, B. 2011. Endo-cannabinergic modulation of IL-1β in mouse hippo-campus under basal conditions and after *in vivo* systemic lipopolysaccharide stimulation. *Neuroimmunomodulation* 18: 226–231.

Cuénod, C. A., Denys, A., Michot, J. L., et al. 1993. Amygdala atrophy in Alzheimer's Disease: An *in vivo* magnetic resonance imaging study. *Arch. Neurol.* 50:941–945.

Drenth, J. P., and van der Meer, J. W. 2001. Hereditary periodic fever. *New Engl. J. Med.* 345:1748–1757.

Emerich, D. F., and Walsh, T. J. 1990. Cholinergic cell loss and cognitive impairments following intraventricular or intradentate injection of colchicine. *Brain Res.* 517:157–167.

Fan, Y., Dutta, J., Gupta, N., Fan, G., et al. 2008. Regulation of programmed cell death by NF-κB and its role in tumorigenesis and therapy. *Adv. Exp. Med. Biol.* 615:223–250.

Fanelli, F., Sepe, S., D'Amelio, M., et al. 2013. Age-dependent roles of peroxisomes in the hippocampus of a transgenic mouse model of Alzheimer's disease. *Mol. Neurodeg.* 8:8.

Figarella, K., Rawer, M., Uzcategui, N. L., et al. 2005. Prostaglandin D_2 induces programmed cell death in *Trypanosoma brucei* bloodstream form. *Cell Death Diff.* 12:335–346.

Ganguly, R., and Guha, D. 2008. Alzheimer's disease and protection by *Moringa oleifera*. *Indian J. Med. Res.* 128:744–751.

Gehrmann, J., Matsumoto, Y., and Kreutzberg, G. W. 1995. Microglia: Intrinsic immune effector cell of the brain. *Brain Res. Rev.* 20: 269–287.

Giuliani, D., Bitto, A., Galantucci, M., et al. 2014. Melanocortins protect against progression of Alzheimer's disease in triple-transgenic mice by targeting multiple pathophysiological pathways. *Neurobiol. Aging* 35: 537–547.

Green, L. C., Wagner, D. A., Glogowski, J., et al. 1982. Analysis of nitrate, nitrite, and [^{15}N]-nitrate in biological fluids. *Anal. Biochem.* 126:131–138.

Jacobs, H. I., van Boxtel, M. P., Jolles, J., et al. 2012. Parietal cortex matters in Alzheimer's disease: An overview of structural, functional and metabolic findings. *Neurosci. Biobehav. Rev.* 36: 297–309.

Ke, J., Long, X., Liu, Y., et al. 2007. Role of NF-κB in TNFα-induced COX-2 expression in synovial fibroblasts from human TMJ. *J. Dent. Res.* 86:363–367.

Koo, E. H., Sisodia, S. S., Archer, D. R., et al. 1990. Precursor of amyloid protein in Alzheimer disease undergoes fast anterograde axonal transport. *Proc. Natl. Acad. Sci. USA* 87:1561–1565.

Kumar, A., Dogra, S., and Prakash, A. 2010. Protective effect of naringin, a citrus flavonoid, against colchicine-induced cognitive dysfunction and oxidative damage in rats. *J. Med. Food* 13:976–984.

Kumar, A., Naidu, P. S., Seghal, N., and Padi, S. S. 2007b. Neuroprotective effects of resveratrol against intra-cerebroventricular colchicine-induced cognitive impairment and oxidative stress in rats. *Pharmacology* 79:17–26.

Kumar, A., Seghal, N., Naidu, P. S., et al. 2007a. Colchicine-induced neuro-toxicity as an animal model of sporadic dementia of Alzheimer's type. *Pharmacol. Rep.* 59:274–283.

Kumar, A., Sehgal. N., Puneet, K., et al. 2008. Protective effect of quercetin against icv colchicine-induced cognitive dysfunctions and oxidative damage in rats. *Phytother. Res.* 22:1563–1569.

Kumar, M. H., and Gupta, Y. K. 2002. Intra-cerebroventricular administration of colchicine produces cognitive impairment associated with oxidative stress in rats. *Pharmacol. Biochem. Behav.* 73:565–571.

Lowry, O. H., Rosebrough, N. J., Farr, A. L., and Randall, R. J. 1951. Protein measurement with Folin phenol reagent. *J. Biol. Chem.* 193: 265–275.

Mallat, M., and Chamak, B. 1994. Brain macrophages: Neurotoxic or neurotrophic effector cells? *J. Leukocyte Biol.* 56:416–422.

Minton, K. 2001. Immune mechanisms in neurological disorders: Protective or destructive? *Trends Immunol.* 22:655–657.

Mizuno, M., Yamada, K., Olariu, A., et al. 2000. Involvement of brain-derived neurotrophic factor in spatial memory formation and maintenance in a Radial Arm Maze test in rats. *J. Neurosci.* 20: 7116–7121.

Mouton, P. R., Martin, L., Calhoun, M., et al. 1998. Cognitive decline strongly correlates with cortical atrophy in Alzheimer's dementia. *Neurobiol. Aging* 19:371–377.

Nolan, Y., Vereker, E., Lynch, A. M., and Lynch, M. A. 2003. Evidence that lipopolysaccharide-induced cell death is mediated by accumulation of reactive oxygen species and activation of p38 in rat cortex and hippocampus. *Exp. Neurol.* 184:794–804.

Nyoman, G., and Darmadipura, S. 2007. Role of microglia as prime component of CNS immune system in acute and chronic neuroinflammation. *Folica Med. Indonesiana* 43:54–58.

Parikh, A. A., Moon, M., Pritts, T., et al. 2000. IL-1β induction of NF-κB activation in human intestinal epithelial cells is independent of oxyradical signaling. *Shock* 13:8–13.

Paxinos, G., and Watson, C., (Eds.). 1986. *The Rat Brain in Stereotaxic Coordinates*. San Diego, CA: Academic Press.

Pitchaimani, V., Arumugam, S., Thandavarayan, R. A., et al. 2012. Nootropic activity of aceta-minophen against colchicine induced cognitive impairment in rats. *Clin. Biochem. Nutr.* 50:241–244.

Rai, S., Kamat, P. K., Nath, C., and Shukla, R. 2013. A study on neuroinflammation and NMDA receptor function in STZ (ICV) induced memory impaired rats. *J. Neuroimmunol.* 254:1–9.

Roy, C. 2014. Role of *Moringa oleifera* on hippocampal cell morphology and senile plaque formation in colchicine induced experimental rat model of Alzeimer's Disease. *Intl. J. Curr. Pharm. Res.* 6:51–54.

Sabuncu, M., Desikan, R., Sepulcre, J., et al. 2011. Dynamics of cortical and hippocampal atrophy in Alzheimer Disease. *Arch. Neurol.* 68: 1040–1048.

Shibli, R. A., Daradkah, N. Q., Makhadmeh, I. M., and Baghdadi, S. H. 2010. Colchicine production from colchicum and the role of *in vitro* cultures: A review. *Jordan. J. Agric. Sci.* 6:208–222.

Shigematsu, K., and McGeer, P. L. 1992. Accumulation of amyloid precursor protein in neurons after intraventricular injection of colchicine. *Am. J. Pathol.* 140:787–794.

Sil, S., Goswami, A. R., Dutta, G., and Ghosh, T. 2014. Effects of naproxen on some immune responses in colchicine induced rat model of Alzheimer's Disease. *Neuroimmunomodulation* 21: 304–321.

Socci, D. J., Bjugstad, K. B., Jones, H. C., et al. 1999. Evidence that oxidative stress is associated with the pathophysiology of inherited hydrocephalus in the H-Tx rat model. *Exp. Neurol.* 155: 109–117.

Stevens, A., and Bancroft, J. D., (Eds.). 1977. Proteins and nucleic acids. In: *Theory and Practice of Histological Techniques*. London: Elsevier, pp. 129.

Streit, W. J. 1993. Microglial-neuronal interactions. *J. Chem. Neuroanat.* 6:261–266.

Terkeltaub, R. A. 2003. Clinical practice. Gout. *New. Engl. J. Med.* 349: 1647–1655.

Trease, G. E., and Evans, W. C., (Eds.). 1989. *Pharmacognosy.* London: Elsevier, pp. 600–603.

Wilson, L. 1986. Microtubules as targets for drug and toxic chemical action: The mechanisms of colchicine and vinblastine. In: *The Cytoskeleton – A Target for Toxic Agents* (Clarkson, T. W., Sagar, P. R., and Syversen, T. L., Eds.). New York: Plenum Press, pp. 37–52.